NIH-PA Author Manuscript

NIH-PA Author Manuscript

NIH-PA Author Manuscript

Targeted estrogen delivery reverses the metabolic syndrome

Brian Finan[1,2,3], **Bin Yang**[3], **Nickki Ottaway**[4], **Kerstin Stemmer**[1,2], **Timo D Müller**[1,2], **Chun-Xia Yi**[1,2], **Kirk Habegger**[4], **Sonja C Schriever**[1,2], **Cristina García-Cáceres**[1,2], **Dhiraj G Kabra**[1,2], **Jazzminn Hembree**[4], **Jenna Holland**[4], **Christine Raver**[4], **Randy J Seeley**[4], **Wolfgang Hans**[5], **Martin Irmler**[5], **Johannes Beckers**[5,6], **Martin Hrabě de Angelis**[5,6], **Joseph P Tiano**[7], **Franck Mauvais-Jarvis**[7], **Diego Perez-Tilve**[4], **Paul Pfluger**[1,2,4], **Lianshan Zhang**[8], **Vasily Gelfanov**[3], **Richard D DiMarchi**[3], and **Matthias H Tschöp**[1,2,4]

[1]Institute for Diabetes and Obesity, Helmholtz Zentrum München, German Research Center for Environmental Health (GmbH), Neuherberg, Germany

[2]Department of Medicine, Division of Metabolic Diseases, Technische Universität München, Munich, Germany

[3]Department of Chemistry, Indiana University, Bloomington, Indiana, USA

[4]Metabolic Diseases Institute, Department of Internal Medicine, Division of Endocrinology, University of Cincinnati College of Medicine, Cincinnati, Ohio, USA

[5]German Mouse Clinic, Institute of Experimental Genetics, Helmholtz Zentrum München, GmbH, Neuherberg, Germany

[6]Chair of Experimental Genetics, Technische Universität München, Freising-Weihenstephan, Germany

[7]Department of Medicine, Comprehensive Center on Obesity, Division of Endocrinology, Metabolism and Molecular Medicine, Northwestern University Feinberg School of Medicine, Chicago, Illinois, USA

[8]Jiangsu Hengrui Medicine Co., Ltd, Jiangsu Province, China

Abstract

We report the development of a new combinatorial approach that allows for peptide-mediated selective tissue targeting of nuclear hormone pharmacology while eliminating adverse effects in other tissues. Specifically, we report the development of a glucagon-like peptide-1 (GLP-1)-estrogen conjugate that has superior sex-independent efficacy over either of the individual hormones alone to correct obesity, hyperglycemia and dyslipidemia in mice. The therapeutic benefits are driven by pleiotropic dual hormone action to improve energy, glucose and lipid

metabolism, as shown by loss-of-function models and genetic action profiling. Notably, the peptide-based targeting strategy also prevents hallmark side effects of estrogen in male and female mice, such as reproductive endocrine toxicity and oncogenicity. Collectively, selective activation of estrogen receptors in GLP-1–targeted tissues produces unprecedented efficacy to enhance the metabolic benefits of GLP-1 agonism. This example of targeting the metabolic syndrome represents the discovery of a new class of therapeutics that enables synergistic co-agonism through peptide-based selective delivery of small molecules. Although our observations with the GLP-1–estrogen conjugate justify translational studies for diabetes and obesity, the multitude of other possible combinations of peptides and small molecules may offer equal promise for other diseases.

Pharmaceutical intervention in chronic diseases often requires a polypharmaceutical approach in which multiple agents individually address specific disease mechanisms. For instance, type 2 diabetes therapy often includes separate drugs targeting insulin resistance and insulin deficiency. However, vast unmet needs remain in diabetes management[1], and anti-obesity drugs with the potential to prevent type 2 diabetes remain elusive. Combination therapies offer promising solutions, and many examples of potentiated efficacy exist, with leptin combination therapy as the paradigm[2,3]. However, combination therapies have their shortcomings as well, including potency matching and regulatory approval. To overcome these inadequacies and challenges, we focused on the discovery of new multifunctional single molecules targeting key pathways governing energy balance and glucose homeostasis.

One of the most effective therapies in the treatment of type 2 diabetes involves activation of the receptor for the gut-derived hormone GLP-1. The metabolic profile of GLP-1 includes incretin and satiety effects that are coordinated through simultaneous actions at multiple targets, including the endocrine pancreas and metabolic control centers in the central nervous system (CNS)[4,5]. Two peptide-based GLP-1 mimetics (exenatide and liraglutide) provide sustained improvements in glycemic control without hypoglycemic liability[6, 7]. Unlike other anti-hyperglycemic therapies, including dipeptidyl peptidase-IV inhibitors, chronic GLP-1 therapy also lowers body weight. Though beneficial, such weight loss rarely exceeds 10% in humans[8] and therefore does not achieve a transformative impact on the global health threat of obesity and type 2 diabetes. Recent attempts to enhance the modest weight-lowering effect of GLP-1 therapy have focused on co-administration strategies[9,10], preferably through the integration of multiple pharmacologies into a single molecule. To this end, we recently reported the generation of single-molecule peptides with balanced GLP-1 and glucagon receptor agonism that efficiently normalize body weight and metabolism in diet-induced obese rodents[11]. Here we report a poly-pharmaceutical approach that does not use the combination of two structurally related peptides but instead is a marriage of peptide and nuclear hormone pharmacologies.

Estrogens are steroid hormones that have been repeatedly implicated as a therapeutic option for obesity and type 2 diabetes[12]. They modulate energy expenditure and feeding behavior through leptinlike effects in the hypothalamus[13-16]. However, the clinical application of estrogens is limited by their gynecological and tumor-promoting actions. One strategy to make estrogens therapeutically more viable is represented by the use of selective estrogen receptor modulators with tissue-specific actions. However, this approach has been difficult to develop, in large part because of remaining toxicity concerns and mechanistic uncertainties[17]. Here we propose an alternative strategy based on a peptide carrier that delivers estrogen selectively to specific tissues. We hypothesized that an improved estrogen action profile can be achieved through GLP-1 receptor (GLP-1R)-mediated cellular targeting and intracellular delivery. We envisioned this approach to synergize with GLP-1 pharmacology while improving the therapeutic index of estrogen. We report the discovery of new GLP-1–based estrogen conjugates with full GLP-1 potency and plasma-stable linkages

to estrogen. Using a series of pharmacological and mechanistic studies, we validated the synergistic ability of such peptide conjugates to maximize the metabolic benefits above those of single agonists without inducing hallmark adverse effects of systemic estrogen action.

RESULTS

In vitro characterization of GLP-1–estrogen conjugates

We synthesized a series of single-molecule GLP-1–estrogen conjugates with a substantial range of GLP-1R potency and varying linker stability. We covalently attached an estrogen to the peptide through an ether bond at the third position of 17β-estradiol (Fig. 1a) or as an aromatic ester at the third position of estrone (Fig. 1b). The parent GLP-1 analog contained (i) a 2-aminoisobutyric acid substitution at the second position to prevent *in vivo* dipeptidyl peptidase-IV inactivation, (ii) addition of the nine-residue C-terminal extension derived from exendin-4 and (iii) addition of a C-terminal lysine amide to serve as the estrogen attachment site. Additionally, to maximize GLP-1 potency, we introduced glutamic acid at the 16th position[11,18] (Supplementary Fig. 1a). The GLP-1 ether and aromatic ester estrogen conjugates had binding affinities (half-maximal inhibitory concentration (IC_{50})) and biochemical signaling potencies (half-maximal effective concentration (EC_{50})) that matched the parent peptides (Supplementary Table 1), which confirmed that estrogen attachment does not appreciably influence the inherent activity of the peptide. The preservation of GLP-1 activity allows for ligand-activated endocytosis of GLP-1R at target cells that provide intracellular transport of the conjugated estrogen to access its intracellular receptors. We prepared a GLP-1 analog of less than 0.01% potency but with native biophysical properties from a comparable sequence composed entirely of D stereochemistry and two alanine substitutions at the 1st and 22nd positions[19] (Supplementary Fig. 1b).

The covalent attachment of estrogen to GLP-1, in ether form, appreciably reduced the ability of estrogen to bind estrogen receptor α (ERα), with a measured IC_{50} approximately 1% that of 17β-estradiol (Supplementary Table 1). However, the two conjugates had different intracellular estrogen receptor activity. The ether conjugate had less than 0.005% of the intracellular estrogen activity that 17β-estradiol did, whereas the aromatic ester conjugate had comparable intracellular estrogen activity to estrone (Supplementary Table 1). The cells used to determine intracellular estrogen activity do not express GLP-1R, essentially mimicking off-target cell populations. This explains the lack of activity with the ether conjugate, as peptides are inherently membrane impermeable, meaning there is no cellular point of entry for the estrogen, which is restricted from accessing its intracellular receptors. This masking of estrogen activity with the subsequent preservation of GLP-1 activity allows GLP-1 pharmacology to deliver estrogen to tissues where the GLP-1R is present. However, the high degree of estrogen activity with the aromatic ester conjugate results from its labile chemical attachment that releases the estrogen extracellularly. This estrogen is subsequently available for uptake and activation of intracellular estrogen receptors.

We determined the chemical stability of the conjugates by incubation under physiological conditions (human plasma, pH 7.4, 37 °C) with HPLC–mass spectrometry analysis. The ether conjugate was stable for well over 120 h (Fig. 1a) and is here termed 'stable GLP-1–estrogen'. The aromatic ester conjugate completely degraded within 6 h to release the estrogen, with an estimated half-life of ~1.5 h (Fig. 1b), and is referred to here as 'labile GLP-1–estrogen'. This labile conjugate behaves similarly *in vivo* to untargeted estrogen and can be used to test systemic estrogen action with or without simultaneous GLP-1 action, depending on the peptide sequence used.

Stable GLP-1–estrogen maximizes metabolic benefits

To determine whether estrogen conjugation provides additional metabolic benefits, we administered both of the conjugates along with the comparative unconjugated GLP-1 control to diet-induced obese (DIO) male mice. The stable GLP-1–estrogen conjugate was more efficacious at lowering body weight in a dose-dependent manner than either the GLP-1 control or the labile GLP-1–estrogen conjugate (Fig. 1c). At the higher dose (400 μg per kg body weight), the GLP-1 control decreased the body weight of the mice by 10.3% (53.9 ± 1.2 g (mean ± s.e.m.) to 48.5 ± 1.5 g, $P < 0.01$, $n = 8$ mice per group), and the labile GLP-1–estrogen conjugate decreased the body weight of the mice by 7.5% (54.1 ± 0.9 g to 50.0 ± 1.1 g, $P < 0.01$), whereas the stable GLP-1–estrogen conjugate resulted in body weight loss (23.8%) that was more than double that caused by either of the other treatments (54.0 ± 1.5 g to 41.2 ± 1.4 g, $P < 0.001$). These results confirmed that the covalent attachment of estrogen to GLP-1 enhances the weight-lowering efficacy of the parent peptide and that a plasma-stable linkage between estrogen and GLP-1 is essential for the additive efficacy.

The decreased body weight induced by the stable conjugate was associated with a decrease in cumulative food intake (Fig. 1d) and body-fat mass (Fig. 1e) compared to the GLP-1 control and labile conjugate without a difference in lean mass (Supplementary Fig. 2a). The decreased adiposity induced by the stable conjugate was reflected in lowered plasma leptin concentrations (Fig. 1f), indirectly suggesting an improvement in leptin sensitivity. The stable conjugate also improved hyperglycemia (Fig. 1g), glycemic control (Fig. 1h), insulin sensitivity (Fig. 1i), dyslipidemia (Fig. 1j), respiratory quotient (Supplementary Fig. 2b), hepatosteotosis and hepatocellular damage (Supplementary Fig. 2c). The stable conjugate did not influence energy expenditure or locomotor activity (Supplementary Fig. 2d). It also did not alter testosterone levels or cause observable testicular atrophy (Supplementary Fig. 2e) despite elevated estradiol-like immunoreactivity in the circulation (Supplementary Fig. 2f), which is attributed to the estradiol that is attached to the peptide rather than *de novo* steroidogenesis, demonstrating that this plasma-stable covalent attachment to a peptide sequesters its systemic actions but does not mask antigen epitopes. We also found similar metabolic improvements in female DIO mice administered the stable conjugate (Supplementary Fig. 3a-e).

The stable conjugate delivers a clear additional efficacy relative to the parent peptide and labile conjugate that is most notable at the higher dose. We then hypothesized that additional efficacy could be gained with facilitated intracellular estrogen release, leading to greater synergistic benefits. Therefore, we generated two unique conjugates specifically designed with different meta-stable linker chemistries, each of which was stable in plasma but degraded more readily in intracellular conditions (Supplementary Fig. 4a-f and Supplementary Table 1). However, these meta-stable conjugates were not superior to the stable conjugate at lowering body weight (Supplementary Fig. 4g,h). Such similar metabolic efficacy of the meta-stable and stable conjugates indicates that the stable ether-based conjugate is sufficiently processed intracellularly and capable of releasing an adequately active estrogen in the target cell.

Though we have yet to fully characterize the moiety released intracellularly, two potential liberated estrogen metabolites (Supplementary Fig. 5) have considerably more estrogen activity than the intact stable conjugate. Despite having an intracellular activity that is less than 1% that of native estradiol (EC_{50} 0.004 ± 0.001 nM (mean ± s.d.)), a lysine adduct that we hypothesized to be liberated from C-terminal proteolysis had a subnanomolar EC_{50} (0.563 ± 0.027 nM) and was nearly 200-fold more active than the intact conjugate (EC_{50} 108.2 ± 15.73 nM) (Supplementary Table 1). Furthermore, estradiol 3-carboxymethyl ether, which we hypothesized to result from hydrolysis of the amide bond linking the lysine to the estrogen, showed substantially greater estrogen response element (ERE)-mediated

transcriptional activity (EC$_{50}$ 0.033 ± 0.018 nM) compared to the aforementioned lysine adduct and had 12% of the activity of estradiol (Supplementary Table 1). We do not expect the intracellularly delivered moiety to be native estradiol because oxidative cleavage of the ether bond is unlikely. Of appreciable importance is the fact that the labile estrogen conjugate at either of the two doses studied did not show additional efficacy compared to treatment with the free GLP-1 peptide. Consequently, we conclude that the enhanced efficacy of the stable conjugate was the result of the concerted activity of GLP-1 and estrogen at the same, specifically targeted anatomical site.

Stable GLP-1–estrogen is devoid of adverse estrogen effects

To determine whether the GLP-1–estrogen conjugates have off-target hypertrophic activity in the uterus, we compared the conjugates in ovariectomized (OVX) lean mice. At a maximal dose of 4,000 μg per kg body weight, neither the GLP-1 control (0.05 ± 0.02 g, $n =$ 8 mice per group) nor the stable conjugate (0.04 ± 0.01 g) led to higher uterine weight above that of saline-treated mice, whereas the labile conjugate (0.10 ± 0.02 g, $P < 0.01$) led to a 2.5-fold higher uterine weight compared to the saline-treated mice (Fig. 2a). The uterine hypertrophy induced by the labile estrogen conjugate reflects the systemic and untargeted effects of free estrogen released from the conjugate, which represents toxicity that limits the therapeutic use of estrogen. The absence of uterotrophic effects with the stable conjugate shows that the chemically stable ether linkage prevents estrogen release and accumulation in plasma, thus eliminating the adverse gynecological action. Furthermore, plasma concentrations of luteinizing hormone and follicle-stimulating hormone (FSH) were not altered by the stable conjugate (Fig. 2b), suggesting that the stable conjugate does not influence the hypothalamic-pituitary-gonadal axis.

To assess the tumorigenic potential of the estrogen conjugates in breast tissue, we monitored the growth of estrogen-dependent MCF-7 xenografts in OVX nude mice. Through the first 21 d after grafting, estradiol stimulated sizeable tumor growth (159.8 ± 27.9 mm^3 (mean ± s.e.m.), $P < 0.001$, $n = 10$ mice per group), as did the labile conjugate at the maximal dose of 4,000 μg per kg body weight (110.5 ± 11.4 mm^3, $P < 0.001$) (Fig. 2c). This further confirms the systemic estrogenic activity of the labile conjugate. In contrast, the stable conjugate did not induce tumor growth during this initial phase (34.1 ± 5.9 mm^3, not significant) (Fig. 2c), verifying that the stable conjugate masks the ability of estrogen to stimulate the growth of hormone-sensitive breast-cancer cells. All mice had measurable tumors through the first 3 weeks after xenograft, indicating that the injected tumor cells had mostly survived *in vivo*. However, tumors in the stable conjugate group were of lower relative size compared to those of the other groups, and most were not measurable after day 21. At day 68, the tumor incidence was 100% in the estradiol and labile-conjugate groups but was only 30% in the stable conjugate-treated mice (Fig. 2d). Harvested tumors in the estradiol group had a weight of 779.7 ± 257.7 mg (mean ± s.e.m., $P < 0.001$) (Fig. 2e) and a volume of 1,461.2 ± 584.3 mm^3 ($P < 0.001$) (Fig. 2f). Though the tumors were smaller and weighed less in the labile conjugate group than in the estradiol group (92.1 ± 23.8 mm^3 and 37.0 ± 9.0 mg, $P < 0.001$ for each measure), they were substantially larger than the tumors that remained in the stable-conjugate group (12.0 ± 6.7 mm^3 and 6.3 ± 0.8 mg, $P < 0.001$ for each measure). Examining the uteri from these nude mice confirmed our earlier observations in C57BL/6 mice showing that stable conjugation to GLP-1 eliminates estrogenic action at reproductive tissues (Fig. 2g). Collectively, the stable covalent attachment of estrogen to GLP-1 prevented the hallmark side effects of estrogen in several rodent models, including reproductive endocrine toxicity and oncogenicity.

Additionally, we examined the off-target estrogenic effects on bone density through dual-energy X-ray absorptiometry and peripheral quantitative computed tomography (pQCT). The dual-energy X-ray absorptiometry analysis did not reveal any estrogen-induced

increases in whole skeletal-bone density after treatment with any of the compounds (Supplementary Table 2). The pQCT analysis revealed a significant increase in the cortical and subcortical content in both the femoral metaphysis ($P < 0.05$) and diaphysis ($P < 0.01$) in the mice treated with the labile conjugate (Supplementary Table 2), which is indicative of the systemic effect of estrogen on bone metabolism. Treatment with the stable conjugate did not result in any of these effects. Notably, these results further demonstrate that the selectivity and specificity gained through GLP-1–mediated targeting is consistent with the extremely limited presence of GLP-1Rs in bone (Supplementary Fig. 6a).

Benefits of GLP-1–estrogen depend on CNS GLP-1R activation

To determine the contribution of GLP-1 to the efficacy of the GLP-1–estrogen conjugates, we generated conjugates composed of a low-potency GLP-1 analog (Supplementary Table 1) and compared them in DIO mice. We studied the labile estrogen conjugate of the weak GLP-1 agonist to establish the efficacy of estrogen divorced from GLP-1 activity or targeting, essentially serving as an aqueous-soluble estrogen prodrug. At the maximal dose of 4,000 μg per kg body weight, the weak GLP-1 agonist-stable estrogen conjugate decreased body weight by 5.1% (50.4 ± 1.6 g to 47.8 ± 1.5 g, $P < 0.001$, $n = 8$ mice per group) (Fig. 3a). This was markedly less than the same conjugate of the high-potency GLP-1 agonist, despite a tenfold higher dose. This result was slightly superior but comparable to the 2.9% reduction in body weight induced by the inactive GLP-1 control (53.3 ± 2.7 g to 51.8 ± 2.6 g, not significant). However, the low GLP-1 potency-labile conjugate reduced body weight by 20.6% (49.8 ± 1.2 g to 39.4 ± 0.9 g, $P < 0.001$) (Fig. 3a), which was attributable to substantial estrogen release to the systemic circulation (Fig. 3b). Parallel improvements in cumulative food intake (Fig. 3c) and plasma lipid concentrations (Fig. 3d) were gained with this labile conjugate, but it had inconclusive effects on blood glucose levels after *ad libitum* feeding (Fig. 3e). The independent effect of estrogen on body weight was clearly visible at doses ~100-fold greater than the physiological concentrations of estrogen, and uterine hypertrophy was also present at this dose (Fig. 3f). At this heightened exposure to free estrogen, we found weight lowering comparable to that previously recorded with 10% the dose of the fully potent stable estrogen conjugate (Fig. 1c), but this result occurred at the cost of hepatocellular damage (Fig. 3g). This validates previously reported observations that estrogen alone can reduce body weight[14,20] but underscores the enhanced metabolic outcomes and safety through GLP-1 targeting.

We used CNS-specific GLP-1R knockout (nestin-Cre *Glp1r*^{−/−}) mice exposed to a high-fat diet to determine whether tissues that contain GLP-1R are responsible for mediating the amplified efficacy of the stable conjugate. Similar to previous results, GLP-1 alone resulted in a modest yet significant 3.6% body weight loss ($P < 0.05$) in wild-type mice fed the high-fat diet after just 3 d of treatment (Fig. 3h). Furthermore, this modest weight loss in wild-type mice was amplified by the stable conjugate at the equivalent dose of 400 μg per kg body weight, which induced an 8.5% decrease in body weight ($P < 0.001$) (Fig. 3h). However, neither GLP-1 nor the stable conjugate induced any weight loss in the nestin-Cre *Glp1r*^{−/−} mice (Fig. 3h). These results, along with a parallel trend in cumulative food intake (Fig. 3i), demonstrate that the metabolic benefits of the stable conjugate are mediated by GLP-1Rs in the CNS. Supporting this conclusion and consistent with a predominantly hypothalamic mode of action, the stable conjugate increased proopiomelanocortin (POMC) and leptin receptor gene expression in the arcuate nucleus to a greater extent than GLP-1 or estrogen agonism alone (Fig. 3j). Systemic estrogen also decreased neuropeptide Y (NPY) gene expression (Fig. 3j), but the stable conjugate did not. These findings, together with the fact that the hypothalamus expresses an abundance of GLP-1 and estrogen receptors (Supplementary Fig. 6a), suggest that GLP-1–mediated estrogen delivery may provide metabolic benefits through hypothalamic POMC neurons.

Benefits of GLP-1–estrogen involve estrogen receptors

We showed that the stable conjugate induces an estrogen-specific signal through *in vitro* cell culture measurements. Stimulation of INS-1E cells with GLP-1 alone did not change gene expression of *Trim25* (encoding zinc-finger protein 147), a known estrogen-inducible gene[21] (Fig. 4a). However, stimulation with estradiol resulted in an increase in expression of *Trim25* in a dose-dependent manner. This result was mirrored after stimulation with the stable conjugate, but to slightly lesser degree (Fig. 4a). Furthermore, gene expression analysis revealed that the stable conjugate stimulated *Trim25* expression in the hypothalamus of DIO mice (1.75-fold relative to vehicle, $P < 0.001$) (Fig. 4b), and this stimulation was significantly greater ($P < 0.001$) than that induced by the labile conjugate (1.36-fold relative to control, $P < 0.001$) (Fig. 4b) and consistent with targeted action. We also confirmed the specific stimulation of *Trim25* expression with the stable conjugate in the arcuate nucleus of chronically treated DIO male mice (Fig. 4c), as well as acutely treated OVX female mice (Supplementary Fig. 6b). However, such an estrogen-specific response derived from the stable conjugate was not evident in the livers of either group (Fig. 4d), a tissue that does not express GLP-1R, but was present in the livers of the groups treated with the labile conjugate. In addition to *Trim25*, treatment with the stable conjugate, but not GLP-1 alone, increased the hypothalamic expression of other known estrogen-responsive genes, including *Htr5b*[22], *Nppa*[23] and *Vav3* (ref. 24) (Supplementary Fig. 6c). Collectively, these results show that in cells that have the appropriate combination of receptors, the stable conjugate is capable of initiating estrogen-specific signaling events. However, the exact relative contributions of ERα, ERβ and G protein–coupled estrogen receptor (GPER) remain to be delineated, as INS-1E cells (data not shown) and hypothalamic tissue express all three (Supplementary Fig. 6a).

We compared the stable conjugate in wild-type, ERα knockout (*Esr1*^{−/−}) and ERβ knockout (*Esr2*^{−/−}) DIO mice to the parent GLP-1 peptide to determine the respective contribution of the estrogen receptors to the action of the stable conjugate. Consistent with previous observations in wild-type DIO mice, the stable conjugate reduced body weight by 23.6% ($P < 0.001$), which is more than double the weight-lowering effect of GLP-1 (10.0%, $P < 0.01$) (Fig. 4e). A similar comparison in *Esr1*^{−/−} mice revealed that the decrease in body weight was 10.2% with GLP-1 ($P < 0.001$) and 15.9% with the stable conjugate ($P < 0.001$) (Fig. 4e). Likewise, in *Esr2*^{−/−} mice, the body weight reduction was 9.9% with GLP-1 ($P < 0.01$) and 14.5% with the stable conjugate ($P < 0.001$) (Fig. 4e). The magnitude of this additional weight loss was blunted in both knockout strains ($\Delta = 5.7\%$ in *Esr1*^{−/−} and $\Delta = 4.6\%$ in *Esr2*^{−/−}) compared to wild-type mice ($\Delta = 13.6\%$) (Fig. 4e). Notably, the action of GLP-1 on body weight in obese wild-type mice and the two genetically silenced strains was similar, but the differential weight-lowering efficacy of the stable conjugate was substantially diminished in both knockout strains. We conclude that estrogen signaling synergizes with GLP-1 action to improve systemic metabolism and that both ERα and ERβ are required for the full estrogen-mediated metabolic benefits that are derived from the stable conjugate. However, we cannot exclude the possibility of GPER fractionally contributing to the estrogenic signaling induced by the stable conjugate.

Benefits do not result from altered pharmacokinetics

The enhanced *in vivo* efficacy attributed to the covalent attachment of estrogen to GLP-1 could derive from an enhancement of the pharmacokinetic profile of GLP-1, possibly by promoting its association with circulating plasma proteins through the attached steroid. In the presence of 20% human plasma, neither GLP-1 nor the stable conjugate resulted in lower *in vitro* GLP-1R potency when compared to the activity in the absence of plasma. However, an acylated GLP-1 analog with an identical peptide sequence but with a γGlu-γGlu-palmitoyl chain instead of estrogen (Supplementary Fig. 7a) yielded a ~400-fold lower

potency because of a sequestration effect (EC_{50} 0.025 ± 0.002 nM without plasma compared to EC_{50} 11.16 ± 0.41 nM with plasma) (Fig. 5a). This *in vitro* finding demonstrates that the estrogen does not influence *in vitro* plasma protein binding in a functionally relevant manner.

To further validate the absence of an altered pharmacokinetic profile *in vivo*, we determined the plasma concentration of each compound after a single injection of the stable conjugate or the comparative peptide control to lean mice. Compared to the GLP-1 control at the maximal dose of 4,000 μg per kg body weight, the stable conjugate resulted in a slightly greater maximal concentration (C_{max}), but the time to maximal concentration (T_{max}) and half-life ($T_{1/2}$) were comparable, and there were no detectable amounts of either peptide 8 h after injection (Fig. 5b,c), but we found comparable profiles for the two peptides at the pharmacological dose of 400 μg per kg body weight. This indicates that the covalent attachment of estrogen to GLP-1 offers little enhancement over the initial exposure and no change in the rate of clearance. To further validate the notion that the beneficial effects of our stable conjugate are not the result of estrogen contributing major changes to the *in vivo* pharmacokinetic profile, we compared the *in vivo* efficacy of the stable conjugate to that of the aforementioned acylated GLP-1 analog and a GLP-1–lithocholic acid conjugate (Supplementary Fig. 7a,b). Lithocholic acid should have a similar effect to estrogen on GLP-1 pharmacokinetics because of its comparable lipophilicity, but lithocholic acid is devoid of the metabolic activity of estrogen. In terms of body weight loss, the acylated GLP-1 significantly outperformed the stable GLP-1–estrogen conjugate (30.1% compared to 22.1% body weight loss, $P < 0.05$, $n = 8$ mice per group), and, in turn, the stable conjugate significantly outperformed the lithocholic acid conjugate (13.1% body weight loss, $P < 0.01$) (Fig. 5d), which had the same effect as free GLP-1. We found a similar trend in food intake (Fig. 5e). The lithocholic acid conjugate was also devoid of estrogen-specific gene expression in the hypothalamus (Fig. 5f) and liver (Fig. 5g). We conclude that these changes are insufficient to attribute altered GLP-1 pharmacokinetics as the primary source of the substantially enhanced efficacy; rather, these data support the notion that the enhanced efficiency is caused primarily by a direct estrogenic effect in GLP-1–targeted cell populations.

To determine whether the potentiation of metabolic benefits by estrogen conjugation is unique to GLP-1, we made stable estrogen conjugates to the structurally related gut peptide hormones glucose-dependent insulinotropic polypeptide (GIP) and glucagon with sub-sequent testing in DIO mice. Similar to previous results, the stable attachment of estrogen to GLP-1 enhanced the weight-lowering (Fig. 5h), anorectic (Fig. 5i) and anti-hyperglycemic (Fig. 5j) effects compared to GLP-1 alone. However, the stable attachment of estrogen to a GIP analog did not potentiate the metabolic benefits to the extent observed with GLP-1. Furthermore, the conjugation of estrogen to glucagon did not induce body weight loss in this 1-week study (Fig. 5h) but did provide differential effects on blood glucose concentrations. The glucagon analog increased blood glucose concentrations after *ad libitum* feeding by 7.8% from baseline (128.8 ± 2.6 mg dl^{-1} to 138.9 ± 2.6 mg dl^{-1}, $P < 0.01$), whereas the glucagon-estrogen conjugate decreased blood glucose concentrations by 15.5% (151.8 ± 3.2 mg dl^{-1} to 128.3 ± 2.4 mg dl^{-1}, $P < 0.001$) (Fig. 5j). These results emphasize the pharmacological virtue of the unique combination of GLP-1 and estrogen while minimizing alternative interpretations pertaining to biophysical, pharmacokinetic or super-agonistic properties.

DISCUSSION

We have identified a new approach to direct specific tissue delivery of nuclear hormones to unique cell subpopulations and discovered the enhanced pharmacology of specific drug

candidates for the treatment of the metabolic syndrome. Our approach uses a biologically active peptide to function as a medicinal chaperone in masking and directing nuclear hormone action with profound specificity in selecting target tissues. The peptide also functions to transport the nuclear hormone across the cellular membrane of targeted cells to deliver the biological effect. Notably, we have demonstrated that a unimolecular peptide plus steroid covalent fusion of a GLP-1 analog with an estrogen molecule was much more effective in reducing adiposity and improving hyperglycemia and dyslipidemia in metabolically compromised obese mice than the individual agonists alone, independent of sex. The therapeutic benefits are characterized by dual hormonal and tissue-targeted action without a change in pharmacokinetic properties. Moreover, targeted GLP-1–estrogen hybrids were remarkably devoid of adverse estrogenic properties, including uterine hypertrophy, testicular atrophy and tumorigenic action in breast tissue, which were evident when estrogen pharmacology was divorced from GLP-1 despite its similar achievements in aberrant metabolism, albeit at higher doses. We believe these findings are a result of the combination of the incretin and satiety effects of GLP-1 combined with the leptin-like properties of estrogen[14] that synergize to decrease body weight beyond what is achieved with either individual component.

A plasma-stable attachment of estrogen is necessary for this amplification, as we found no additional efficacy using attachment of estrogen to a fully potent GLP-1 analog by chemistry that is unstable to physiological conditions, resulting in the plasma release of active estrogen. We propose that the diminished activity of the labile conjugate results from the disseminated action of estrogen caused by its premature and nonspecific release to the circulation and its consequential failure to deliver sufficient estrogen action to specific target tissues. Additionally, the presence of full GLP-1 potency in the conjugate is essential, as demonstrated by the absence of efficacy in the stable estrogen conjugate comprised of a poorly potent GLP-1 analog. Furthermore, this synergistic efficacy is driven by central GLP-1 action, as CNS-specific deletion of GLP-1R rescinds the efficacy to that of peripheral GLP-1 alone. Thus, we conclude the GLP-1 component of the conjugate is required to (i) contribute its known beneficial effects to energy balance and insulin secretion, (ii) deliver the estrogen to desired target tissues and transport the attached estrogen intracellularly and (iii) sequester estrogen from systemic action at undesired hormone-sensitive tissues.

The enhanced weight-lowering efficacy of the stable GLP-1–estrogen conjugate seems to be mediated through central effects on energy homeostasis, particularly food intake, with perhaps minor thermogenic qualities. Mice consistently eat less food after treatment with the stable conjugate. They also use more calories from fat, as reflected in a decreased respiratory quotient and a correlative decrease in free fatty acid levels, but it cannot be ruled out that this decrease is the consequence solely of reduced food intake. The robust effects on food intake, in combination with the loss of efficacy in CNS-specific GLP-1R knock-out mice, imply mediation by GLP-1R-expressing cell populations in the hypothalamus, brainstem or both[5] that also coexpress estrogen receptors. The precise neuroanatomical functions and sites of action remain to be fully characterized. Our results suggest that the synergistic efficacy may be propagated through selective estrogen action in GLP-1R-containing POMC neurons in the arcuate nucleus as opposed to NPY neurons or actions in the ventromedial hypothalamus[16], as the negative energy balance seems to be dominated by anorectic mechanisms without substantial modulation of energy expenditure or spontaneous physical activity. Moreover, our results suggest that the conjugate may attenuate leptin resistance, perhaps at the transcriptional level. In accordance with the leptinomimetic effect of estrogen, determining the leptin dependence of the metabolic efficacy of GLP-1–estrogen and the prospect of convergence with leptin signaling is of interest.

In addition to its unique and enhanced metabolic efficacy, the stable conjugate is remarkably devoid of classical estrogen action in hormone-responsive reproductive tissues in both sexes. This property of estrogen has deterred investigation and application of estrogen for chronic diseases. Collectively, the lack of gynecological-, mitogenic- or skeletal-system effects provides a convincing demonstration of the targeted nature of this combinatorial peptide-estrogen conjugation strategy and a sizable increase in the therapeutic index for the use of estrogen. Nevertheless, the biggest remaining safety concern is the prospect of tumorigenic enhancement in any cell that bears both sets of receptors and responds to both hormones, and the conjugate will need to be carefully studied in appropriately powered, long-term toxicology studies. Although hypothetical, thyroid C cell hyperplasia[25,26] and insulinoma are subjects of such concerns. Specifically, GLP-1 stimulates proliferation of pancreatic β cells[4], and estrogen protects β cells from apoptosis[27-29]. However, a controlled mitogenic effect on pancreatic β cells may represent a welcome pharmacological addition to diabetes treatment. In addition to protective effects in the islets, estrogen has been implicated in the direct regulation of insulin biosynthesis in pancreatic islets[30]. We speculate that estrogen could enhance the insulinotropic actions of GLP-1 in the islets similarly to its weightloss enhancing effects and therefore may have curative potential for type 2 diabetes, as it targets several underlying pathological mechanisms—adiposity, insulin resistance and insulin deficiency[12].

We investigated the mechanism of enhanced activity and individual component contributions of the stable conjugate by indirect and direct means. The fact that estrogen and GLP-1 are independently capable of improving body weight and glucose control renders it challenging to determine the contributions of each individually. The necessity of GLP-1–mediated central targeting was shown using chemical and genetic loss-of-function studies. The treatment of obese estrogen-receptor knock-out mice demonstrated the contributions of the individual isoforms but was not decisive in terms of revealing all of the molecular mechanisms that are potentially involved in conjugate-based estrogen signaling. The stable conjugate had a blunted efficacy compared to wild-type mice, suggesting that neither ERα nor ERβ dominate in mediating the enhanced pharmacology of the stable conjugate. However, it is possible that the conjugate signals through alternative or compensatory estrogen signaling mechanisms in these knockout mice[31,32] or through GPER, which may be involved in metabolic control[33,34]. Clearly, our understanding of estrogen pharmacology continues to evolve, and in a comparative sense, the limitations in defining the molecular mechanisms in differential selective estrogen receptor modulator pharmacology illustrates the complexities in characterizing state-of-the-art molecules. Though the specific molecular mechanism of the estrogenic pharmacology in our conjugate has yet to be elucidated, classically defined estrogen-mediated transcriptional events are initiated in GLP-1R-positive target cells and tissues by the stable conjugate. Neither the stable conjugate nor the potential intracellular estrogen metabolites have the maximal *in vitro* cellular potency of native estrogens, yet the estrogenic activity in targeted tissues *in vivo* was markedly amplified compared to that of systemic estrogen. We attribute this phenomenon to GLP-1–mediated targeting, which can enhance the localized estrogen concentration, deliver estrogen to privileged sites (cellular or subcellular) where endogenous estrogens may not have access or a combination of the two. The continued discovery of additionally relevant molecular mechanisms is an ongoing undertaking that is justified by these *in vitro* and *in vivo* observations.

We explored the comparative pharmacology of pharmacokinetically enhanced peptides featuring an acyl chain or lithocholic acid, as well as stable GIP and glucagon conjugates with estrogen, to assess alternative mechanisms potentially contributing to the enhanced efficacy. The initial concern that the enhanced efficacy resulted from prolonged pharmacokinetics was addressed through a demonstration of no change in activity when

studied *in vitro* in the presence of plasma, which was consistent with the subtle *in vivo* differences in PK measurements. We also showed that estrogen does not prolong the *in vivo* duration of action to the extent that acylation does. Moreover, the addition of lithocholic acid, a moiety with a similar lipophilic character as estrogen without the metabolic activity of estrogen that has independently been reported to sustain the action profile of exendin-4 (ref. 35), did not enhance GLP-1 pharmacology. Collectively, these results corroborate that estrogen does not enhance the pharmacokinetics of GLP-1. Alternatively, stable estrogen linkage to glucagon showed less change in body weight relative to linkage to GLP-1, but there was a notable difference in glycemia. The subtle increase in glucose derived by glucagon was reversed by the glucagonestrogen conjugate without a difference in body weight. The inability to potentiate the pharmacology of glucagon to decrease body weight suggests that glucagon mediates delivery to cells that are unresponsive to the anorectic effects of estrogen; however, more studies are required to draw a definitive conclusion. If the attached estrogen simply creates peptide super-agonists or radically enhances the duration of action, then we would expect to see a potentiation of the weight-lowering and enhanced-diabetogenic effects of glucagon instead of a reversal of glycemic pharmacology. As the glucagon-estrogen conjugate improves glycemic control, we speculate that estrogen is targeted to the liver to counteract glucagon-induced hepatic gluconeogenesis or glycogenolysis. These results are worthy of further investigation, as well as an extension to conjugates for which the peptide has inherent mixed agonism within the B class of G protein–coupled receptors. However, broader peptide agonism would result in a dispersal of the estrogen to more tissues, which may dilute the metabolic efficacy gained by selective agonism and increase the potential for adverse effects.

A final point worthy of discussion pertains to the intracellular mechanism of action. Our work demonstrates that the stable conjugate can initiate classical ERE-mediated transcriptional events, but we cannot exclude a contribution from signaling through rapid cytosolic cascades that are analogous to estrogen-dendrimer conjugates[36]. In the initial design of an ideal GLP-1–estrogen conjugate, we believed unique meta-stable chemical linkers (plasma stable and intracellular labile) would be required to achieve intracellular estrogen signaling. However, it was informative that conjugates that were purposefully designed to release an active estrogen only under intracellular conditions were equal, but not superior, in efficacy to the physiologically stable ether conjugate. We suspect that all of these conjugates that are stable in plasma are processed intracellularly to release a more potent estrogen, albeit perhaps with less potency than native estrogens, and the added complexity in the synthesis of selectively stable conjugates is not a necessity to achieve enhanced efficacy and safety. This concept is plausible and consistent with several examples of non-cleavable linker chemistries used in antibody–cytotoxic drug conjugates, including trastuzumab emtansine (T-DM1)[37]. The proposed release mechanism of the cytotoxic payload DM1 involves lysosomal processing of the antibody to liberate a lysine-DM1 adduct that retains its cytotoxic potency but is unable to escape from its targeted cell to surrounding cells[38]. We hypothesize that an analogous mechanism may govern the intracellular processing of the stable GLP-1–estrogen conjugate, and this parallel highlights that similarly to T-DM1, the stable conjugate is dependent on retention of activity in the modified cargo after release as well as the inherent physiology of the targeted cell.

In conclusion, we report a new concept combining both a polypharmacy approach for treating metabolic diseases and the targeted delivery of nuclear hormones, thus laying a foundation for translational pursuit of our GLP-1–estrogen conjugate but also for the conceptual expansion to other molecular combinations. Selective peptide targeting of thyroid hormone to increase basal metabolism or ignite brown fat thermogenesis[39] while avoiding adverse cardiovascular effects may offer an alternative to challenging attempts at tailoring receptor isoform–selective small molecules. Another possibility is to deliver the

anti-inflammatory effects of glucocorticoids to specific tissues involved in metabolic diseases, such as adipose tissue, liver and/or hypothalamus[40], to provide unique health benefits without their diabetogenic effect. In summary, the pharmacological concept presented here holds appreciable promise for a range of new therapies by exploiting the well-recognized pharmacology of nuclear hormones and peptides in a synergistic and targeted fashion.

ONLINE METHODS

Peptide synthesis and cleavage

We synthesized peptides by solid-phase peptide synthesis methods using *in situ* neutralization for both tert-butyloxycarbonyl (Boc)-based and fluorenylmethoxycarbonyl (Fmoc)-based chemistries. For Boc-based neutralization peptide synthesis, we used 0.2 mmol 4-methylbenzhydrylamine (MBHA) resin (Midwest Biotech) on a highly modified Applied Biosystems 430A peptide synthesizer by standard Boc methods using 3-(diethoxyphosphoryloxy)-1,2,3-benzotriazin-4-(3H)-one (DEPBT)/N,N-diisopropylethylamine (DIEA) for coupling and trifluoroacetic acid (TFA) for deprotection of N-terminal amines. We treated peptidyl resins with hydrofluoric acid and *p*-cresol (10:0.5 (v/v)) at 0 °C for 1 h with agitation. We removed the hydrofluoric acid *in vacuo* and precipitated the cleaved and deprotected peptide in diethyl ether. For Fmoc-based neutralization peptide synthesis, we used 0.1 mmol Rink MBHA resin (Novabiochem) on an Applied Biosystems 433A peptide synthesizer by standard Fmoc methods using diisopropylcarbodiimide (DIC)/6 Cl–HOBt for coupling and 20% piperidine and dimethylformide (DMF) for deprotection of N-terminal amines. We treated completed peptidyl resins with TFA, triisopropylsilane (TIS) and anisole (9:0.5:0.5 (v/v/v)) for 2 h with agitation. After removal of the ether, we dissolved the crude peptide in aqueous buffer containing at least 20% acetonitrile (ACN) and 1% acetic acid (AcOH) before lyophilization. We confirmed the peptide molecular weights by electrospray ionization (ESI) mass spectrometry and confirmed their character by analytical reversed-phase (HPLC in 0.1% TFA with an ACN gradient on a Zorbax C8 column (0.46 cm × 5 cm).

Derivatization of estrogen for conjugate containing an ether bond

For both classes of the peptide-estrogen conjugates, we derivatized estrogen in solution to contain both the desired linker chemistries and chemistries used to covalently couple the estrogen to the orthogonally deprotected side-chain amine of the C-terminal lysine amide on the peptidyl resin. To synthesize the derivatized estrogen for constructing the ether conjugate, we reacted estradiol 17-acetate (Sigma) and a tenfold excess of ethyl 2-bromoacetate (Sigma) in dioxane with a presence of K_2CO_3 under reflux conditions and agitation for 48 h, during which we monitored the reaction progress by analytical reversed-phase HPLC as described above. After removal of dioxane *in vacuo*, we resuspended the intermediate product in dioxane with 1 N NaOH for 2 h with heat to remove both the acetyl group protecting the 17th position of the estrogen and the ethyl group capping the derivatized third position of the estrogen. After removal of dioxane *in vacuo*, we acidified the crude product with HCl and dichloromethane (DCM). After the removal of DCM *in vacuo*, we resuspended the crude product in aqueous solvent containing at least 20% methanol, 20% ACN and 1% AcOH and lyophilized it. We purified the crude extract by reversed-phase HPLC in 0.1% TFA with an ACN gradient on a Vydac C8 column (2.2 cm × 25 cm), and we confirmed its molecular weight by ESI mass spectrometry.

Derivatization of estrogen for conjugate containing an aromatic ester bond

We mixed estrone (Sigma) and a tenfold excess of succinic anhydride in DMF with 5% DIEA and 4-dimethylaminopyridine (DMAP) for 48 h at room temperature, during which

we monitored the reaction progress by analytical reversed-phase HPLC as described above. After the removal of DMF *in vacuo*, we extracted the crude product with ethyl acetate washed with aqueous HCl (0.01 N). After the removal of ethyl acetate *in vacuo*, we resuspended the crude product in aqueous solvent containing at least 20% methanol, 20% ACN and 1% AcOH and lyophilized it. We purified the crude extract by reversed-phase HPLC in 0.1% TFA with an ACN gradient on a Vydac C8 column (2.2 cm × 25 cm), and we confirmed its molecular weight by ESI mass spectrometry.

Peptide-estrogen conjugate syntheses

We synthesized the peptide back-bones as described above and conjugated the estrogen on the peptidyl resins. For both classes of conjugates described here, we covalently added the derivatized estrogen to the side-chain amine on the C-terminal lysine amide residue. For peptide backbones synthesized using Boc-based neutralization chemistry, we used a C-terminal Lys(Fmoc)-OH residue, whose side chain was orthogonally deprotected with two 15-min treatments with 20% piperidine and DMF, for the site of estrogen attachment. For peptide backbones synthesized using Fmoc-based neutralization chemistry, we used a C-terminal N'-methyltrityl-L-lysine (Lys(Mtt)-OH) residue, whose side chain was orthogonally deprotected with four 10-min treatments with 1.5% TFA, 2% TIS and 1% anisole in DMF, for the site of estrogen attachment. We attached the estrogen through the side-chain amine of the C-terminal lysine after treatment with a threefold excess of the purified derivatized estrogen and DIC/6 Cl-HOBt in N-methyl-2-pyrrolidone (NMP) for 3–6 h. We confirmed estrogen attachment by ninhydrin analysis. We primarily synthesized the peptide-estrogen conjugates via Fmoc-based neutralization chemistry methods because the hydrofluoric acid cleavage conditions required for Boc-based neutralization chemistry methods resulted in the removal of the 17th-position hydroxyl. After TFA cleavage as described above, we resuspended the crude extract in aqueous buffer containing 20% ACN and 0.1 M NH_4HCO_3 instead of 1% AcOH to facilitate the removal of the TFA adduct formed on the free 17th-position hydroxyl of the estrogen during the cleavage procedure. Similar orthogonal procedures were used to make the GLP-1–lithocholic acid conjugate and the GLP-1–palmitate conjugate.

Peptide and conjugate purification

After cleavage from the resin, we purified crude extracts by semipreparative reversed-phase HPLC in 0.1% TFA with an ACN gradient on a Vydac C8 column (2.2 cm × 25 cm). We purified the peptide–labile estrogen (aromatic ester) conjugates by semipreparative reversed-phase HPLC in 0.025 M NH_4HCO_3 with an ACN gradient on a Phenomenex Luna C5 column (2.2 cm × 25 cm) because the linker chemistry is subject to hydrolysis under acidic conditions. We analyzed preparative fractions for purity by analytical reversed-phase HPLC using the conditions described above. We confirmed peptide molecular weights using ESI mass spectrometry. We lyophilized, aliquoted and stored the purified peptides and conjugates at 4 °C.

Conjugate degradation analysis

We monitored the stability of the conjugates in various incubation conditions using analytical reversed-phase HPLC and ESI mass spectrometry analyses. For chemical stability, we dissolved conjugates (1 mg/ml) in PBS at acidic pH (pH 4.0), neutral pH (pH 7.4) or basic pH (pH 11.0), as well as in cell culture media (DMEM), and incubated them at 37 °C for the duration of the study. We removed aliquots of the incubated conjugates at time points throughout the incubation ranging from 30 min to 120 h and analyzed them by reversed-phase HPLC using the conditions indicated above. We determined the remaining concentrations and estimated half-lives from an AUC analysis. We confirmed the molecular weights and identities of the degraded products by ESI mass spectrometry or matrix-assisted

laser desorption/ionization time-of-flight (MALDI-TOF) mass spectrometry. For plasma stability analysis, we dissolved conjugates (1 mg/ml) in 100% human plasma (Production) and incubated them at 37 °C for the duration of the study. We withdrew aliquots of the incubated conjugates at time points throughout the incubation ranging from 30 min to 120 h and added ACN to precipitate the plasma proteins. We removed precipitates by microcentrifugation before reversed-phase HPLC and mass spectroscopy analysis.

GLP-1R activation

We tested each peptide and conjugate for its ability to activate GLP-1R using a cell-based luciferase reporter gene assay that indirectly measures cyclic AMP (cAMP) induction. We co-transfected human embryonic kidney (HEK 293) cells with GLP-1R complementary DNA (zeocin-selection) and a luciferase reporter gene construct fused to a cAMP response element (CRE) (hygromyocin B–selection). We seeded cells at a density of 22,000 cells per well and serum deprived them for 16 h in DMEM (HyClone) supplemented with 0.25% (v/v) bovine growth serum (BGS) (HyClone). We added serial dilutions of the peptides and conjugates to 96-well cell culture–treated plates (BD Biosciences) containing the serum-deprived, co-transfected HEK 293 cells, and we incubated them for 5 h at 37 °C and 5% CO_2 in a humidified environment. To stop the incubation, we added an equivalent volume of Steady Lite HTS luminescence substrate reagent (Perkin Elmer) to the cells to induce lysis and expose the lysates to luciferin. We agitated the plate for 5 min and stored it for 10 min in the dark. We measured luminescence on either a MicroBeta-1450 liquid scintillation counter (Perkin-Elmer) or a DTX-880 multimode detector (Beckman Coulter). We graphed luminescence data against the concentration of the peptide, and we calculated EC_{50} values using Origin software (OriginLab).

GLP-1R competitive binding

We measured *in vitro* relative binding affinity to GLP-1R through a competitive binding assay using scintillation proximity technology. We prepared receptor membrane fractions from cell lysates of HEK 293 cells co-transfected with GLP-1R. We determined the total protein concentration of the membrane preparations using a bicinchoninic acid (BCA) protein quantification kit (Thermo Fisher Scientific). We incubated serial dilutions of peptides or conjugates with GLP-1R membrane preparations (0.5–5.0 μg per well), a constant concentration of $[I^{125}]$-GLP-1 (Amersham Biosciences) and polyethyleneimine (PEI)-treated wheat germ-agglutinin-coated scintillation proximity assay beads (Amersham Biosciences) in a 96-well plate for 12 h at room temperature. We measured scintillation (counts per second) on a MicroBeta-1450 liquid scintillation counter at both 6 h and 12 h time points. We extrapolated the percentage of specific binding data using total binding and nonspecific binding controls, and we graphed it against concentration of the competitor ligands. We calculated IC_{50} values using Origin software.

Estrogen receptor activation

Each conjugate was tested for its ability to activate ERα and ERβ using a cell-based luciferase reporter gene assay that directly measures induction of ERE. T47D-KBLuc cells were purchased from the American Type Culture Collection (ATCC). This specialized cell line is T47D human breast cancer cells that were stably transfected with a triplet ERE-promoter-luciferase reporter gene construct (G418-selection). Cells were seeded at a density of 80,000 cells per well and serum deprived for 16 h in DMEM supplemented with 0.25% (v/v) BGS. Serial dilutions of estrogen derivatives and conjugates were added to 96-well cell culture–treated plates containing the serum-deprived T47D-KBLuc cells and incubated for 24 h at 37 °C and 5% CO_2 in a humidified environment. To stop the incubation, an equivalent volume of Steady Lite HTS luminescence substrate reagent was added to the cells to induce lysis and expose the lysates to luciferin. The plate was shaken for 5 min at 800

r.p.m. and stored for 10 min in the dark. Luminescence was measured on either a MicroBeta-1450 liquid scintillation counter or a DTX-880 multimode detector. Luminescence data were graphed against the concentration of the peptide, and EC_{50} values were calculated using Origin software.

ERα competitive binding

We measured *in vitro* the relative binding affinity to ERα through a competitive binding assay using phosphorimaging technology. We incubated serial dilutions of estrogen derivatives or conjugates with purified ERα (Invitrogen) (1.5 nM) and $[I^{125}]$-estradiol (PerkinElmer) (0.05 nM) in a 96-well plate for 2 h at room temperature. After the incubation, we transferred the binding cocktail to a 96-well HTS filter plate precoated with 0.25% PEI (Millipore) and filtered and washed the plate five times with binding buffer. We wrapped the dried filter plate in cellophane and exposed it to a phosphorimaging screen for 48 h before scanning it on a Typhoon 9210 image scanner (Amersham Biosciences). We extrapolated the percentage of specific binding data using total binding and nonspecific binding controls, and we graphed it against the concentration of the competitor ligand. We calculated IC_{50} values using Origin software.

Mice

DIO mice—We fed C57/B6 mice (Jackson Laboratories) a diabetogenic diet (Research Diets), which is a high-sucrose diet with 58% kcal from fat. We single- or group-housed the mice on a 12-h light, 12-h dark cycle at 22 °C with free access to food and water.

OVX mice—We ovariectomized wild-type or DIO C57/B6 mice at approximately 9 months of age. We anesthetized the mice with isoflurane. We performed the ovariectomy through a bilateral skin incision made from the first to the third lumbar vertebra in the abdominal cavity. We carefully isolated, ligated and removed the ovaries. We closed the incision in two layers and gave the mice post-operative analgesics.

ERα ($Esr1^{-/-}$) and ERβ ($Esr2^{-/-}$) knockout DIO mice—We fed $Esr1^{-/-}$ and $Esr2^{-/-}$ mice from a C57/B6 genetic background (Jackson Laboratories) a diabetogenic diet (Research Diets), which is a high-sucrose diet with 58% kcal from fat.

CNS-specific GLP-1R conditional knockout mice—We generated mice with *loxP* sites flanking exons 6 and 7 of the GLP-1R gene and crossed them with mice that express Cre recombinase driven by the rat nestin promoter (Jackson Labs). Homozygous mice were used for the pharmacological studies with littermates that were hemizygous for nestin-Cre and wild-type for the GLP-1R as controls. Tissue expression profiles are shown in Supplementary Figure 6d.

All animal studies were approved by the Institutional Animal Care and Use Committees at the University of Cincinnati Office in accordance with the US National Institutes of Health guide for the care and use of laboratory animals.

Pharmacological and metabolism studies

We administered compounds by daily subcutaneous injections. We measured body weight and food intake every other day after the first injection.

Body composition measurements

We measured whole-body composition (fat and lean mass) using nuclear magnetic resonance technology (EchoMRI).

Energy balance physiology measurements

We assessed energy intake and expenditure, as well as home-cage activity, using a combined indirect calorimetry system (TSE Systems). We measured oxygen consumption and carbon dioxide production every 45 min for a total of 120 h (including 12 h of adaptation) to determine the respiratory quotient and energy expenditure. We determined food intake continuously for 120 h at the same time as the indirect calorimetry assessments by integration of scales into the sealed cage environment. We determined home-cage locomotor activity using a multidimensional infrared light-beam system with beams scanning the bottom and top levels of the cage and expressed activity as the number of beam breaks.

Plasma and serum parameters

Blood was collected after euthanasia using EDTA-coated Microvette tubes (Sarstedt), chilled on ice and centrifuged at 3,000g and 4 °C. Individual samples were analyzed. Plasma concentrations of insulin, leptin, estradiol, testosterone and thyroxine were quantified by ELISA assays from commercially available kits (Alpco). Plasma concentrations of luteinizing hormone and FSH were quantified by ELISA assays from commercially available kits (Cusabio). Plasma concentrations of cholesterol, triglycerides, free fatty acids, ALT and AST were measured by enzymatic assay kits (Thermo Fisher). All assays were performed according to the manufacturer's instructions.

Glucose tolerance test and insulin tolerance test

For the determination of glucose tolerance and insulin sensitivity, we subjected the mice to 6 h of fasting and intraperitoneally injected them with either 2 g glucose per kg body weight (20% (wt/v) D glucose (Sigma) in 0.9% (wt/v) saline) for the glucose tolerance test or 1 U insulin per kg body weight (0.1 U/ml; Humolog Pen, Eli Lilly) for the insulin tolerance test. We measured tail blood glucose concentrations (mg dl^{-1}) using a handheld glucometer (TheraSense Freestyle) before (0 min) and at 15, 30, 60, 90 and 120 min after injection.

Tumor growth in MCF-7 xenograft mice

We housed OVX female athymic NCr *nu/nu* mice aged 5–6 weeks (NCRNU-F, Taconic Farms) in positive individual ventilated (PIV) cages under standard conditions and fed them with phytoestrogen-free chow (Teklad Laboratory Animal Diets) throughout the whole experiment. We implanted a subset of the mice ($n = 10$) with a subcutaneous 17β-estradiol–sustained release pellet (0.72 mg per pellet; Innovative Research, Sarasota, FL). We assigned the mice to three dose groups ($n = 10$ per each group). Each of two groups received daily subcutaneous injections of either the stable GLP-1–estrogen or labile GLP-1–estrogen conjugate (4,000 µg per kg body weight), and the third group (subcutaneously implanted with 17β-estradiol release pellets) received daily injections of saline vehicle. After 3 d of injections, we initiated xenografts by a subcutaneous injection of 6×10^7 MCF-7 human estrogen receptor-positive breast cancer cells (ATCC) into the left flank. We maintained MCF-7 cells in ATCC formulated Eagle's Minimum Essential Medium (EMEM) supplemented with 20 µg/ml gentamycin, 5 µg/ml bovine insulin and 10% FBS. We grew cells for inoculation into nude mice to 80% confluence. We trypsinized and resuspended them in a mixture of Matrigel (BD Biosciences) and serum- and antibiotic-free EMEM (1:1) and kept them on ice until injection. As soon the first measurable tumor occurred (day 6 after tumor cell inoculation), we monitored tumor volumes weekly by digital caliper measurement of the length, width and height. We calculated tumor volume using the formula volume = (length × width^2) × π/6, assuming the third diameter to be equal to the shorter of the two measured.

Skeletal analysis

Skeletal analysis was performed in the Bone and Cartilage Module of the German Mouse Clinic. Bone parameters were analyzed using a pDEXA Sabre X-ray Bone Densitometer (Norland Medical Systems) with a scan speed of 20 mm s^{-1}, a resolution of 0.5 mm × 1.0 mm and a histogram average width setting of 0.020 g cm^{-2}. pQCT analysis was carried out using a Stratec XCT Research SA+ (Stratec). The spatial resolution was set to 70 μm, and the distal femoral metaphysis and diaphysis of the left femur from each mouse were examined to obtain volumetric bone mineral density, content and area of the trabecular, cortical and total bone. The periosteal and endosteal circumferences were also evaluated by scanning. The reference line for the computed tomography scans was set at the most distal point of the femur. At 3.0 mm proximal from the reference line, two slices were taken at 0.2 mm intervals, and at 6.0 mm proximal from the reference line, one slice was taken in the femoral diaphysis.

In vivo pharmacokinetic measurements

We administered single subcutaneous injection doses of the peptides at 400 μg per kg body weight and 4,000 μg per kg body weight to lean mice. We collected blood by cardiac puncture from the left ventricle, aorta or inferior vena cava within 24 h before peptide administration and at 15 and 30 min and 1, 4, 8, 12, 24, 48 and 72 h after administration. We mixed samples with K_2-EDTA and kept them on ice. We separated plasma samples by centrifugation and kept them frozen after preparation. We determined concentrations by HPLC–tandem mass spectrometry analyses on a Sciex API-5500 mass spectrometer with positive ESI analysis coupled with a Shimadzu HPLC system on a HyperClone (Phenomenex) C18 column (2.0 cm × 50 mm) with mobile phase gradients. The multiple reaction monitoring transition was m/z (mass-to-charge ratio) 524.4–1,048.4 for the GLP-1 analog and m/z 1,126.5–1,223.2 for the stable conjugate. We calculated peak-area integrations using Analyst software (Applied Biosystems). The calibration curve reached a range of 0.5–200 ng/ml.

In vitro and *ex vivo* gene expression analysis

Each compound was tested for its ability to stimulate estrogen-inducible gene expression through quantitative PCR analysis *in vitro* after a 6 h stimulation period in cultured INS-1E cells or *in vivo* 2–6 h after the final injection after 14 d of administration in DIO mice. INS-1E cells at semiconfluence were incubated with serial dilutions of the compounds in phenol red–free, serum-deprived conditions for 6 h before lysis, and mRNA extraction was performed using RNeasy Mini Kits (Qiagen). Dissected tissues were immediately frozen on dry ice, and RNA was extracted as described above. Between 12 and 16 pieces of microdissected hypothalamic nuclei were captured by laser extraction using a LMD7000 (Leica) laser microscope system, and RNA was extracted using Arcturus Paradise Plus Kits (Invitrogen). After subsequent DNase treatment, 1 μg of mRNA was reverse transcribed using SuperScript III (Invitrogen) and oligo(dT20) primers (Invitrogen). Real-time quantitative PCR analysis was performed on a ViiA7 cycler (Applied Biosystems) using TaqMan assays (Life Technologies). Target gene expression was normalized to β-actin (*Actb*) or *Hprt* and calculated relative to saline vehicle-treated controls.

Statistical analyses

We performed all statistical analyses using GraphPad Prism. We performed the analyses of the results obtained in the *in vitro and in vivo* experiments using one- or two-way ANOVA followed by Tukey's, Bonferroni's or Dunnet's *post hoc* tests. $P < 0.05$ was considered significant. The results are presented as means ± s.e.m. of 4–10 replicates per group. Receptor activation and binding data is ± s.d.

Supplementary Material

Refer to Web version on PubMed Central for supplementary material.

References

1. Grundy SM. Drug therapy of the metabolic syndrome: minimizing the emerging crisis in polypharmacy. Nat. Rev. Drug Discov. 2006; 5:295–309. [PubMed: 16582875]

2. Roth JD, et al. Leptin responsiveness restored by amylin agonism in diet-induced obesity: evidence from nonclinical and clinical studies. Proc. Natl. Acad. Sci. USA. 2008; 105:7257–7262. [PubMed: 18458326]

3. Müller TD, et al. Restoration of leptin responsiveness in diet-induced obese mice using an optimized leptin analog in combination with exendin-4 or FGF21. J. Pept. Sci. 2012; 18:383–393. [PubMed: 22565812]

4. Drucker DJ. The biology of incretin hormones. Cell Metab. 2006; 3:153–165. [PubMed: 16517403]

5. Barrera JG, Sandoval DA, D'Alessio DA, Seeley RJ. GLP-1 and energy balance: an integrated model of short-term and long-term control. Nature reviews. Endocrinology. 2011; 7:507–516.

6. Cvetkovi RS, Plosker GL. Exenatide: a review of its use in patients with type 2 diabetes mellitus (as an adjunct to metformin and/or a sulfonylurea). Drugs. 2007; 67:935–954. [PubMed: 17428109]

7. Davies MJ, Kela R, Khunti K. Liraglutide—overview of the preclinical and clinical data and its role in the treatment of type 2 diabetes. Diabetes Obes. Metab. 2011; 13:207–220. [PubMed: 21205109]

8. Amori RE, Lau J, Pittas AG. Efficacy and safety of incretin therapy in type 2 diabetes: systematic review and meta-analysis. J. Am. Med. Assoc. 2007; 298:194–206.

9. Talsania T, Anini Y, Siu S, Drucker DJ, Brubaker PL. Peripheral exendin-4 and peptide YY$_{3-36}$ synergistically reduce food intake through different mechanisms in mice. Endocrinology. 2005; 146:3748–3756. [PubMed: 15932924]

10. Williams DL, Baskin DG, Schwartz MW. Leptin regulation of the anorexic response to glucagon-like peptide-1 receptor stimulation. Diabetes. 2006; 55:3387–3393. [PubMed: 17130484]

11. Day JW, et al. A new glucagon and GLP-1 co-agonist eliminates obesity in rodents. Nat. Chem. Biol. 2009; 5:749–757. [PubMed: 19597507]

12. Mauvais-Jarvis F. Estrogen and androgen receptors: regulators of fuel homeostasis and emerging targets for diabetes and obesity. Trends Endocrinol. Metab. 2011; 22:24–33. [PubMed: 21109497]

13. Musatov S, et al. Silencing of estrogen receptor α in the ventromedial nucleus of hypothalamus leads to metabolic syndrome. Proc. Natl. Acad. Sci. USA. 2007; 104:2501–2506. [PubMed: 17284595]

14. Gao Q, et al. Anorectic estrogen mimics leptin's effect on the rewiring of melanocortin cells and Stat3 signaling in obese animals. Nat. Med. 2007; 13:89–94. [PubMed: 17195839]

15. Gao Q, Horvath TL. Cross-talk between estrogen and leptin signaling in the hypothalamus. Am. J. Physiol. Endocrinol. Metab. 2008; 294:E817–E826. [PubMed: 18334610]

16. Xu Y, et al. Distinct hypothalamic neurons mediate estrogenic effects on energy homeostasis and reproduction. Cell Metab. 2011; 14:453–465. [PubMed: 21982706]

17. Nilsson S, Koehler KF, Gustafsson JA. Development of subtype-selective oestrogen receptor-based therapeutics. Nat. Rev. Drug Discov. 2011; 10:778–792. [PubMed: 21921919]

18. Patterson JT, et al. A novel human-based receptor antagonist of sustained action reveals body weight control by endogenous GLP-1. ACS Chem. Biol. 2011; 6:135–145. [PubMed: 20939591]

19. Adelhorst K, Hedegaard BB, Knudsen LB, Kirk O. Structure-activity studies of glucagon-like peptide-1. J. Biol. Chem. 1994; 269:6275–6278. [PubMed: 8119974]

20. Bryzgalova G, et al. Mechanisms of antidiabetogenic and body weight-lowering effects of estrogen in high-fat diet-fed mice. Am. J. Physiol. Endocrinol. Metab. 2008; 295:E904–E912. [PubMed: 18697913]

21. Inoue S, et al. Genomic binding-site cloning reveals an estrogen-responsive gene that encodes a RING finger protein. Proc. Natl. Acad. Sci. USA. 1993; 90:11117–11121. [PubMed: 8248217]

22. Papageorgiou A, Denef C. Estradiol induces expression of 5-hydroxytryptamine (5-HT) 4, 5-HT5, and 5-HT6 receptor messenger ribonucleic acid in rat anterior pituitary cell aggregates and allows prolactin release via the 5-HT4 receptor. Endocrinology. 2007; 148:1384–1395. [PubMed: 17122082]

23. Jankowski M, Rachelska G, Donghao W, McCann SM, Gutkowska J. Estrogen receptors activate atrial natriuretic peptide in the rat heart. Proc. Natl. Acad. Sci. USA. 2001; 98:11765–11770. [PubMed: 11562484]

24. Lee K, et al. Vav3 oncogene activates estrogen receptor and its overexpression may be involved in human breast cancer. BMC Cancer. 2008; 8:158. [PubMed: 18518979]

25. Bjerre Knudsen L, et al. Glucagon-like peptide-1 receptor agonists activate rodent thyroid C-cells causing calcitonin release and C-cell proliferation. Endocrinology. 2010; 151:1473–1486. [PubMed: 20203154]

26. Cho MA, et al. Expression and role of estrogen receptor α and β in medullary thyroid carcinoma: different roles in cancer growth and apoptosis. J. Endocrinol. 2007; 195:255–263. [PubMed: 17951536]

27. Le May C, et al. Estrogens protect pancreatic β-cells from apoptosis and prevent insulin-deficient diabetes mellitus in mice. Proc. Natl. Acad. Sci. USA. 2006; 103:9232–9237. [PubMed: 16754860]

28. Liu S, et al. Importance of extranuclear estrogen receptor-α and membrane G protein-coupled estrogen receptor in pancreatic islet survival. Diabetes. 2009; 58:2292–2302. [PubMed: 19587358]

29. Tiano JP, et al. Estrogen receptor activation reduces lipid synthesis in pancreatic islets and prevents β cell failure in rodent models of type 2 diabetes. J. Clin. Invest. 2011; 121:3331–3342. [PubMed: 21747171]

30. Wong WP, et al. Extranuclear estrogen receptor-α stimulates NeuroD1 binding to the insulin promoter and favors insulin synthesis. Proc. Natl. Acad. Sci. USA. 2010; 107:13057–13062. [PubMed: 20616010]

31. Shughrue PJ, Askew GR, Dellovade TL, Merchenthaler I. Estrogen-binding sites and their functional capacity in estrogen receptor double knockout mouse brain. Endocrinology. 2002; 143:1643–1650. [PubMed: 11956145]

32. Park CJ, et al. Genetic rescue of nonclassical ERα signaling normalizes energy balance in obese Erα-null mutant mice. J. Clin. Invest. 2011; 121:604–612. [PubMed: 21245576]

33. Revankar CM, Cimino DF, Sklar LA, Arterburn JB, Prossnitz ER. A transmembrane intracellular estrogen receptor mediates rapid cell signaling. Science. 2005; 307:1625–1630. [PubMed: 15705806]

34. Mårtensson UE, et al. Deletion of the G protein-coupled receptor 30 impairs glucose tolerance, reduces bone growth, increases blood pressure, and eliminates estradiol-stimulated insulin release in female mice. Endocrinology. 2009; 150:687–698. [PubMed: 18845638]

35. Son S, et al. Preparation and structural, biochemical, and pharmaceutical characterizations of bile acid-modified long-acting exendin-4 derivatives. J. Med. Chem. 2009; 52:6889–6896. [PubMed: 19827752]

36. Harrington WR, et al. Estrogen dendrimer conjugates that preferentially activate extranuclear, nongenomic versus genomic pathways of estrogen action. Mol. Endocrinol. 2006; 20:491–502. [PubMed: 16306086]

37. Krop IE, et al. Phase I study of trastuzumab-DM1, an HER2 antibody-drug conjugate, given every 3 weeks to patients with HER2-positive metastatic breast cancer. J. Clin. Oncol. 2010; 28:2698–2704. [PubMed: 20421541]

38. Erickson HK, et al. Antibody-maytansinoid conjugates are activated in targeted cancer cells by lysosomal degradation and linker-dependent intracellular processing. Cancer Res. 2006; 66:4426–4433. [PubMed: 16618769]

39. López M, et al. Hypothalamic AMPK and fatty acid metabolism mediate thyroid regulation of energy balance. Nat. Med. 2010; 16:1001–1008. [PubMed: 20802499]

40. Thaler JP, et al. Obesity is associated with hypothalamic injury in rodents and humans. J. Clin. Invest. 2012; 122:153–162. [PubMed: 22201683]
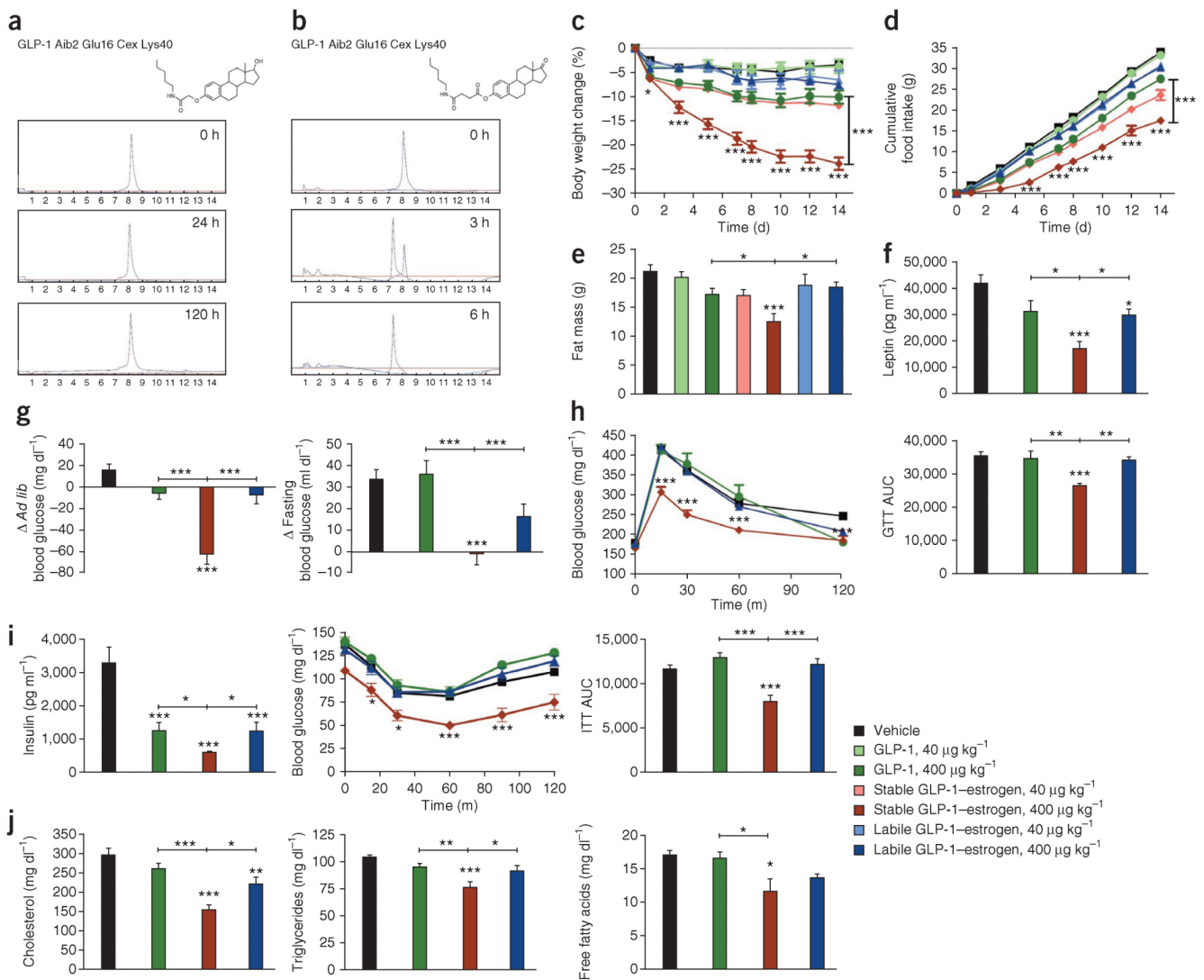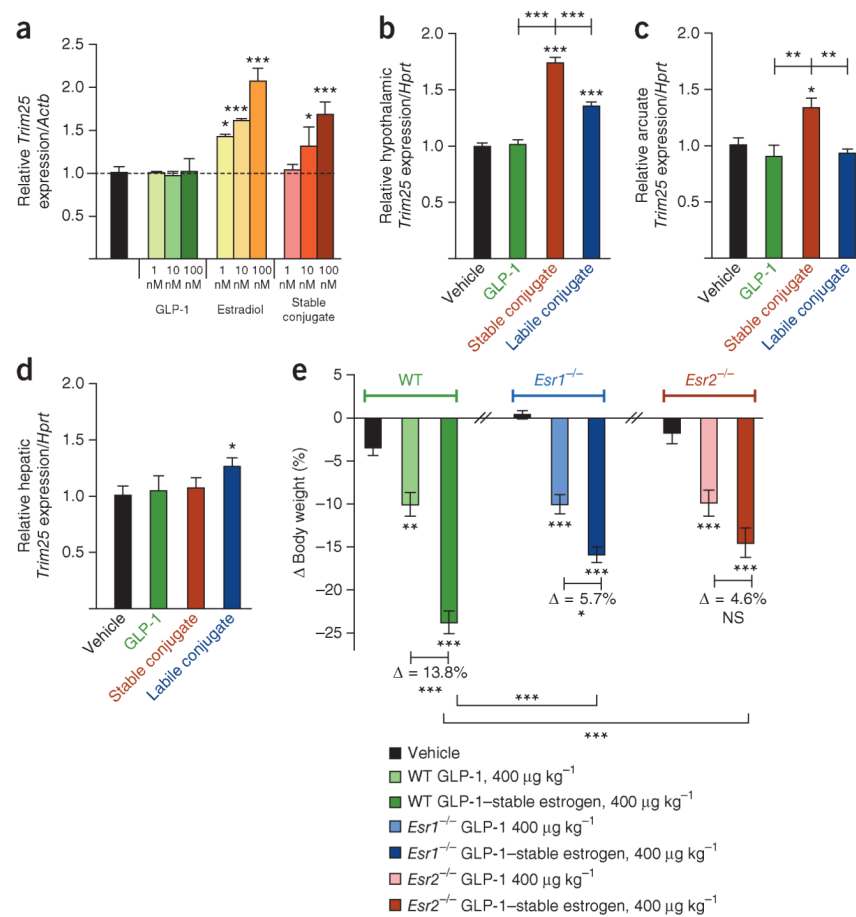
Figure 1.
Two-week treatment of DIO male mice with GLP-1–estrogen conjugates. (**a**) Structure and physiological stability profile of the stable GLP-1–estrogen conjugate featuring an ether bond linkage to estrogen. (**b**) Structure and physiological stability profile of the labile GLP-1–estrogen conjugate featuring a phenolic ester bond linkage to estrogen. (**c–e**) Effects on body weight (**c**), cumulative food intake (**d**) and fat mass (**e**) ($n = 8$ mice per group) after daily subcutaneous injections of a GLP-1 analog (green), the stable GLP-1–estrogen conjugate (red) or the labile GLP-1–estrogen conjugate (blue) at two different doses, 40 μg per kg body weight (lighter shade) and 400 μg per kg body weight (darker shade). (**f–j**) Plasma leptin concentrations (f), *ad libitum* (*ad lib*) and fasted blood glucose concentrations (**g**), intraperitoneal glucose tolerance (**h**), plasma insulin and insulin tolerance after glucose challenge (**i**) and total plasma concentrations of cholesterol, triglycerides and free fatty acids (**j**) in separate experiments after 2 weeks of treatment with the GLP-1 analog, stable conjugate or labile conjugate at the higher dose ($n = 8$ per group). ITT, insulin tolerance test; AUC, area under the curve. Data in a–h represent the means ± s.e.m. *$P < 0.05$, **$P < 0.01$, ***$P < 0.001$ by analysis of variance (ANOVA) comparing saline vehicle to compound injections unless otherwise noted.
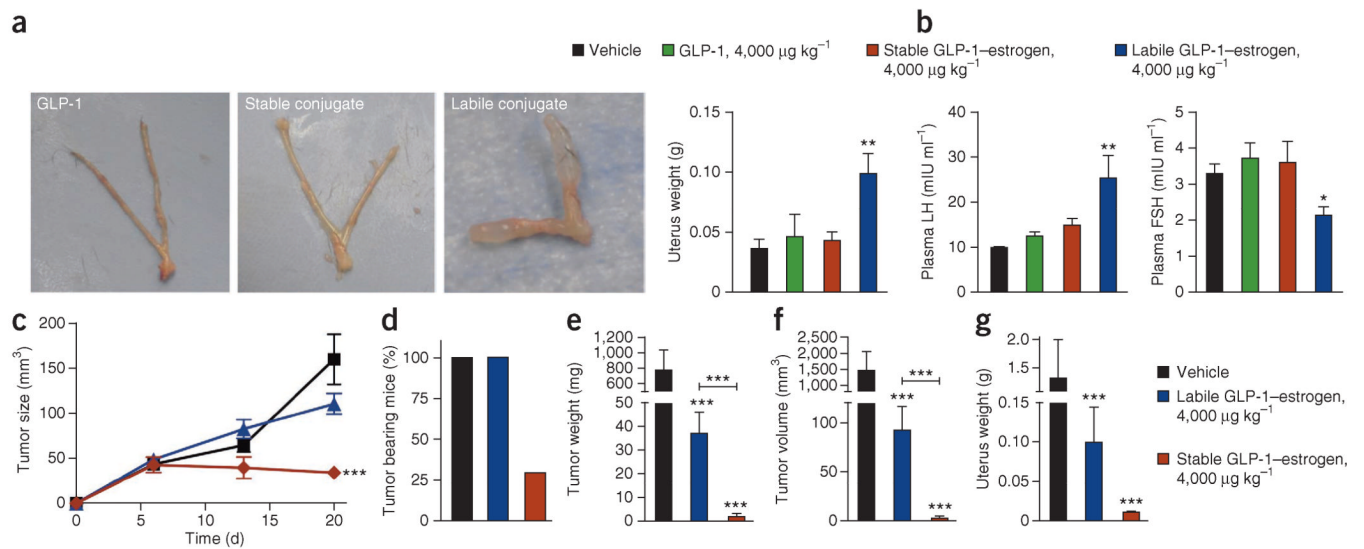
Figure 2.
Uterotrophic and mitogenic effects of GLP-1–estrogen conjugates. (**a,b**) Effects on uterus weight with representative images of extracted uteri (**a**) and plasma concentrations of luteinizing hormone (LH) and FSH (**b**) from OVX mice treated with vehicle (black), GLP-1 analog (green), the stable GLP-1–estrogen conjugate (red) or the labile GLP-1–estrogen conjugate (blue) after daily subcutaneous injections at the maximal dose of 4,000 μg per kg body weight ($n = 8$ female mice per group). (**c**) Effects on subcutaneous MCF-7 xenograft tumor size, as monitored by weekly digital caliper measurements, through 3 weeks of treatment with subcutaneous implantation of an estradiol pellet (black, with subsequent daily injections of saline vehicle) or daily injections of the labile GLP-1–estrogen conjugate (blue) or the stable GLP-1–estrogen conjugate (red) at the maximal dose of 4,000 μg per kg body weight ($n = 10$ female mice per group). (**d–g**) Final tumor-bearing rate (**d**), tumor weight (**e**), volume of extracted tumors (**f**) and uterus weight (**g**) after 9 weeks of treatment. $*P < 0.05$, $**P < 0.01$, $***P < 0.001$ by ANOVA comparing vehicle to compound injections unless otherwise noted. Data in **b,c** and **e–g** are the means $\pm$. s.e.m.
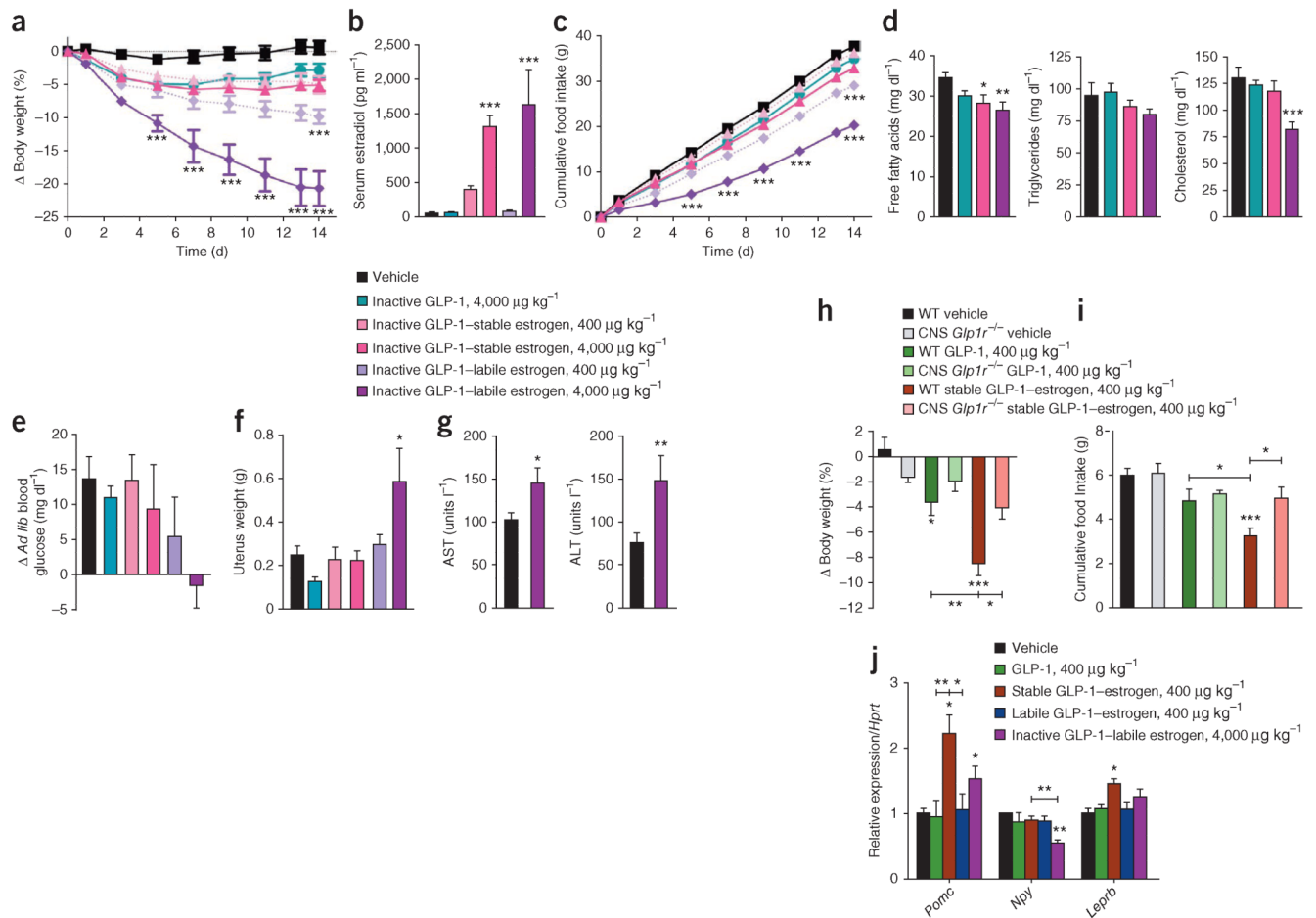
Figure 3.
Metabolic effects of estrogen conjugates to a low-potency GLP-1 analog and the CNS-specific effects of the GLP-1–estrogen conjugates. (**a–g**) Effects on body weight (**a**), serum estradiol concentration (**b**), cumulative food intake (**c**), serum free fatty acid concentration, triglycerides and total cholesterol (**d**), blood glucose concentration after *ad libitum* (*ad lib*) feeding (**e**), uterus weight (**f**) and serum ratio of aminotransferase to alanine aminotransferase (AST/ALT) (**g**) ($n = 8$ female mice per group) after daily subcutaneous injections of vehicle (black), the inactive, D-amino acid GLP-1 analog (teal), inactive stable GLP-1–estrogen conjugate at either 400 μg per kg body weight (salmon) or at 4,000 μg per kg body weight (fuschia) or inactive labile GLP-1–estrogen conjugate at either 400 μg per kg body weight (light purple shade) or at 4,000 μg per kg body weight (dark purple shade). (**h,i**) Effects on body weight (**h**) and cumulative food intake (**i**) ($n = 6$ male mice per group) after three consecutive daily subcutaneous injections in to wild-type mice and mice with CNS-specific ablation of GLP-1R (*Glp1$^{-/-}$*), both exposed to a high-fat diet, with the GLP-1 analog (dark and light green) or the stable GLP-1–estrogen conjugate (red and salmon) at a dose of 400 μg per kg body weight (**j**) Effects on gene expression in microdissected arcuate nuclei from male mice in a separate experiment treated daily with subcutaneous injections of a GLP-1 analog (green), the stable GLP-1–estrogen conjugate (red) or the labile GLP-1–estrogen conjugate (blue) at a dose of 400 μg per kg body weight or with the inactive labile GLP-1–estrogen conjugate (purple) at a dose of 4,000 μg per kg body weight. Data represent the means ± s.e.m. *$P < 0.05$, **$P < 0.01$, ***$P < 0.001$ by ANOVA comparing vehicle to compound injections unless otherwise noted.

Figure 4.
In vitro and *in vivo* assessment of estrogen-specific signaling readouts. (**a**) Dose-dependent fold induction of *Trim25* mRNA relative to a housekeeping gene (*Actb*) in INS-1E cells after incubation with a GLP-1 analog (shades of green), 17β-estradiol (shades of yellow-orange) or the stable GLP-1–estrogen conjugate (shades of red). (**b-d**) Effects in a separate experiment on the fold induction of *Trim25* mRNA relative to a housekeeping gene (*Hprt*) from extracted hypothalamus (**b**), microdissected arcuate nuclei (**c**) and liver (**d**) from male DIO mice treated with daily subcutaneous injections for 2 weeks with GLP-1 analog (green), the stable GLP-1–estrogen conjugate (red) or the labile GLP-1–estrogen conjugate (blue) at a dose of 400 µg per kg body weight. (**e**) Effects on body weight after 2 weeks of daily subcutaneous injections of a GLP-1 analog (lighter shade) or the stable conjugate (darker shade) at a dose of 400 µg per kg body weight in age-matched and body weight-matched wild-type (green), *Esr1*$^{-/-}$ (blue) and *Esr2*$^{-/-}$ mice (salmon-red) ($n = 8$ mice per group). All data represent the means ± s.e.m. *$P < 0.05$, **$P < 0.01$, ***$P < 0.001$ by ANOVA comparing saline control to compound stimulation *in vitro* or vehicle to compound injections independently in each different strain *in vivo* unless otherwise noted.
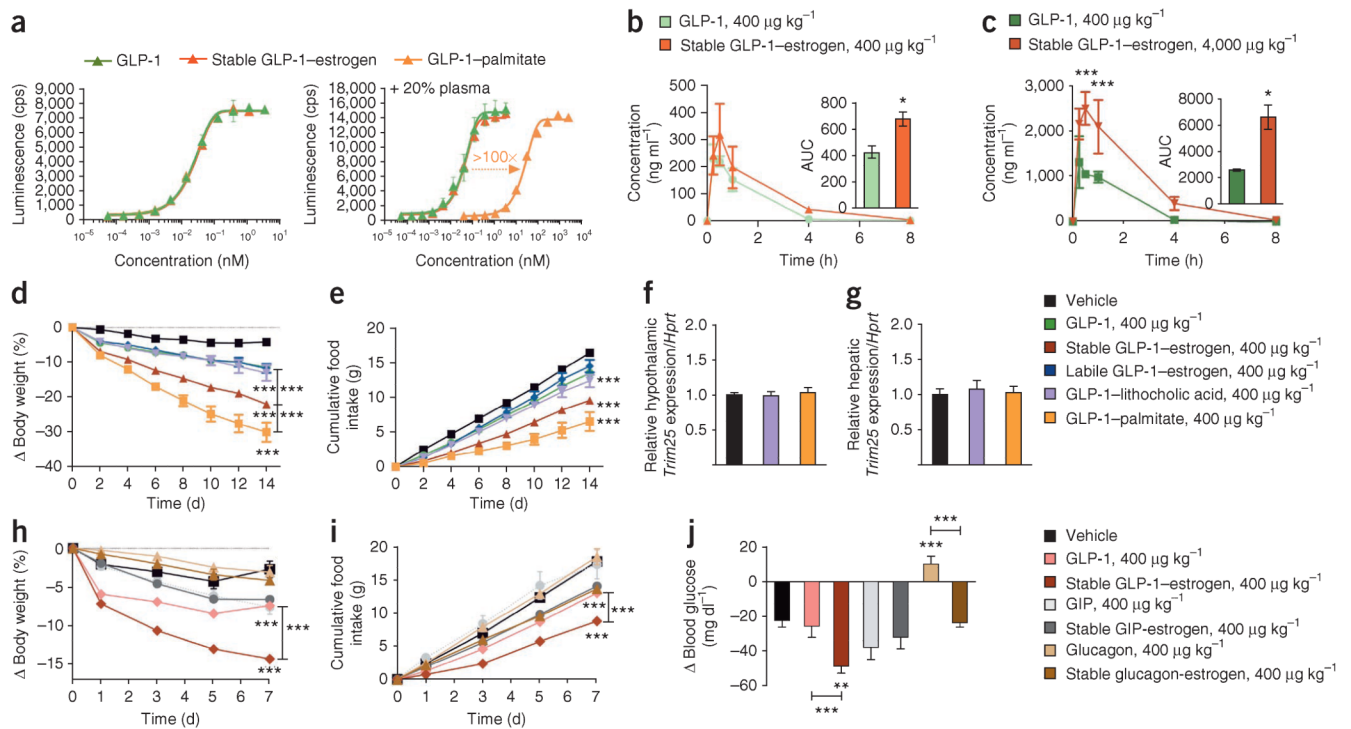
Figure 5.

In vitro and *in vivo* pharmacokinetic profile of the stable GLP-1–estrogen conjugate and comparative efficacy to alternative combinations of peptides and nuclear hormones. (**a**) Dose-response curves for *in vitro* GLP-1R activation in the absence of human plasma (left) and the presence of 20% human plasma (right) of a GLP-1 analog (green) and the stable GLP-1–estrogen conjugate (red) compared to the acylated GLP-1 control (orange). A minimum of three separate experiments were conducted for each compound with or without human plasma. Data in a are means ± s.d. (**b,c**) *In vivo* plasma concentrations and the AUC (insets), as measured by a mass spectrometry-based analysis, of the GLP-1 analog and stable conjugate at a dose of 400 µg per kg body weight (**b**) and the maximal dose of 4,000 µg per kg body weight (**c**) after a single subcutaneous injection in lean mice ($n = 9$ male mice per group). (**d,e**) Effects on body weight (**d**) and cumulative food intake (**f**) ($n = 8$ male mice per group) in a separate experiment after daily subcutaneous injections of a GLP-1 analog (green), the stable GLP-1–estrogen conjugate (red), the labile GLP-1–estrogen conjugate (blue), the GLP-1–lithocholic acid conjugate (violet) or GLP-1–palmitate (yellow-orange) at a single dose of 400 µg per kg body weight for 14 d. (**f,g**) Effects on the fold induction of *Trim25* mRNA relative to a housekeeping gene (*Hprt*) from extracted hypothalamus (**f**) and liver (**g**) of treated mice. (**h–j**) Effects on body weight (**h**), cumulative food intake (**i**) and *ad lib* blood glucose concentration (**j**) ($n = 8$ mice per group) in a separate experiment after daily subcutaneous injections of a GLP-1 analog (salmon), the stable GLP-1–estrogen conjugate (red), a GIP analog (light gray), the GIP-stable estrogen conjugate (dark gray), a glucagon analog (light brown) or the glucagon-stable estrogen conjugate (dark brown) at a dose of 400 µg per kg body weight. Data in *b–j* represent the means ± s.e.m. *$P < 0.05$, **$P < 0.01$, ***$P < 0.001$ by ANOVA comparing compound injections to vehicle unless otherwise noted.